

Microphone System Response in High Amplitude
Noise Environments

Troy Taylor

A senior thesis submitted to the faculty of
Brigham Young University
in partial fulfillment of the requirements for the degree of
Bachelor of Science

Kent Gee, Advisor

Department of Physics and Astronomy
Brigham Young University

August 2011

Copyright © 2011 Troy Taylor

All Rights Reserved

ABSTRACT

Microphone System Response in High Amplitude Noise Environments

Troy Taylor

Department of Physics and Astronomy

Bachelor of Science

The acoustic field near large-scale solid rocket motors represents a harsh, high-amplitude noise environment rich with high-bandwidth acoustic shocks. Type-1 prepolarized microphones may be used in these environments with the benefit of reduced cost and measurement because they require only a constant-current supply available in many data acquisition systems. However, there are potential issues related to microphone response that should be considered. The main issue discussed here has to do with temporary failure of the constant-current supply due to an insufficiently fast response time in representing rapid voltage changes at shocks, which results in spurious, capacitive-like effects in the waveform data that are also manifest as a low-frequency roll-up in the spectrum noise floor. An experiment was conducted to identify under what circumstances these waveform effects arise. Data were measured from a solid rocket motor using several combinations of transducer, cable type, cable length and constant current supply. Results and mitigation methods found from the experiment are discussed. These include increasing the supply current, using low-impedance cables, and choosing the correct orientation for the transducers.

ACKNOWLEDGEMENTS

I would like to acknowledge my advisor, Dr. Kent Gee, for all the time he put into this project. I would also like to acknowledge the Department of Physics and Astronomy for financial assistance provided. I would also like to thank Jarom Giraud and Curtis Wiederhold for helping with the field test and assisting in my data analysis. I especially want to thank my wife for her support during my time working on this project.

Contents

| | |
|--|----|
| Table of Contents | iv |
| List of Figures | v |
| 1 Background | 1 |
| 1.1 Introduction | 1 |
| 1.2 Prepolarized Piezoelectric Microphones | 3 |
| 2 Field Test | 10 |
| 2.1 Equipment and Setup | 10 |
| 2.2 The Firing | 15 |
| 3 Results and Analysis | 20 |
| 3.1 The Data | 20 |
| 3.2 Analysis | 22 |
| 4 Conclusion | 28 |
| Bibliography | 30 |

List of Figures

| | |
|--|----|
| 1.1 Shock example | 1 |
| 1.2 Shock with bad data | 1 |
| 1.3 Maximum frequency with longer cable lengths..... | 6 |
| 1.4 Discharge curve | 7 |
| 1.5 RC high-pass filter | 8 |
| 1.6 Orion-50 power spectral density (PSD)..... | 9 |
| 2.1 Microphone holder | 11 |
| 2.2 Two microphones oriented differently at a shock..... | 12 |
| 2.3 Setup diagram | 14 |
| 2.4 Layout diagram | 16 |
| 2.5 Relative humidity on test day | 17 |
| 2.6 Air pressure on test day..... | 17 |
| 2.7 Wind speed and direction on test day | 18 |
| 2.8 Test pad and setup picture..... | 19 |
| 3.1 Station 1 PSD..... | 21 |
| 3.2 Station 2 PSD..... | 21 |
| 3.3 Station 3 PSD..... | 22 |
| 3.4 Adjacent microphones at a shock | 24 |
| 3.5 Probes from the Orion-50 test..... | 26 |

Chapter 1

Background

1.1 Introduction

With the development of next-generation space programs, new rocket vehicles have been developed and currently are in development. These developments have sparked a renewed desire for knowledge in source characterization and near-field propagation models of rocket noise. Brigham Young University has been commissioned to develop an energy-based acoustic probe suitable for these rocket noise fields[1]. Some microphone systems have shown problems in previous tests done by the Acoustics Research Group at Brigham Young University while testing probes in the noise fields of an Orion-50 rocket motor as well as a Kinetic Energy Interceptor (KEI) Stage 1 motor. These problems occur when a shock occurs in the noise field and the system cannot provide enough instantaneous power to accurately record the shock. The system then saturates. Figure 1.1 shows a typical pressure waveform measured from a KEI Stage 2 rocket motor test during a shockwave recorded on four different channels at the same location. Figure 1.2 shows the data measured from the

same rocket test but on four channels at a different location. Some of these channels show the typical pressure waveform of a shockwave, like seen in Figure 1.1.

However, the red curve saturated at the shockwave. It shows a capacitive-like effect where after the shock it dips below the other data and rises back up to it over time.

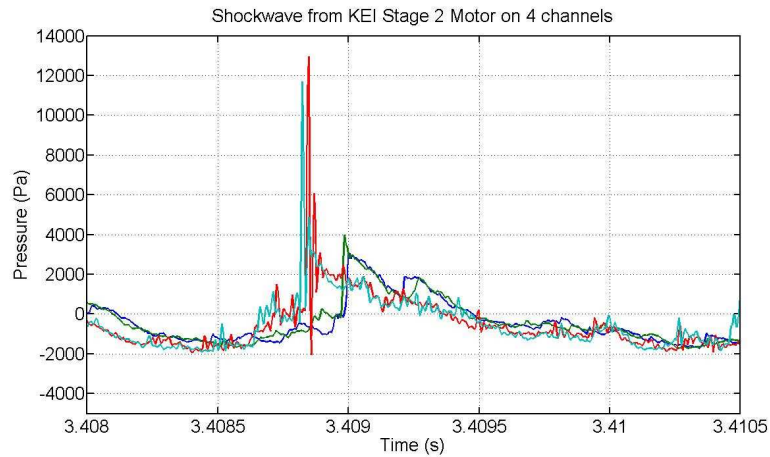


Figure 1.1 A recorded shockwave from a KEI Stage 2 rocket motor test firing. Two of the channels have a higher peak pressure because they were oriented towards the rocket plume, while the other two were pointed upwards

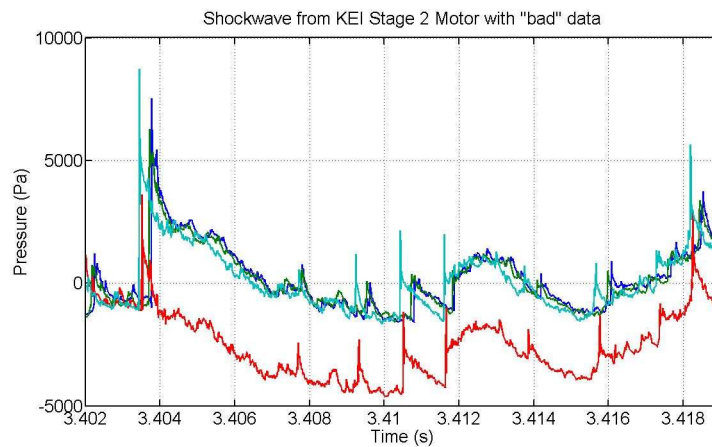


Figure 1.2 Example of a shockwave where one of the sensors recorded bad data. All four sensors recorded data at the same location, but the red curve underestimates the pressure at the shock and for a short time afterwards

A test was carried out in the presence of a KEI Stage 2 solid rocket motor noise field to better understand why these capacitor-like effects are appearing in the data, to establish a change in voltage threshold for when saturation occurs, and to determine guidelines on how the problem can be avoided in future tests. Several different microphone systems were tested, using several combinations of transducer, cable type, cable length and constant current supply.

1.2 Prepolarized Piezoelectric Microphones

Two types of condenser microphones were used in the KEI test. The first type, an externally-polarized condenser microphone, uses a stretched membrane, the diaphragm, separated a small distance from a rigid plate. A polarization voltage is applied between the plate and the diaphragm by an external source. When the pressure from a sound wave acts on the diaphragm, the resulting displacements of the membrane change the capacitance between it and the plate. An output voltage is then created proportional to the displacements of the membrane[2]. The other type of microphone is the prepolarized condenser microphone. It operates the same way as the externally polarized microphone, except it uses an electret, a polarized piece of plastic aluminized on the surface. It doesn't need an external source to provide polarization[2].

Some prepolarized microphones use piezoelectric circuitry. The manufacturer of the microphones we use, GRAS, refers to these microphones as IEPE, which they

will be referred to in this paper. They are also known as ICP[3]. IEPE microphones have several advantages that have made them increasingly popular recently[4]. They are easier to use than an externally-polarized microphone because they don't require a polarization voltage supply but rather can be powered from a constant current source, commonly available from the data acquisition system that it is connected to.

IEPE microphones also have very low output impedance, usually less than 100 Ω . This means that longer cable lengths can be used without a loss of signal[3]. This is ideal when testing in rocket noise fields where generally very long cable lengths are required.

All IEPE microphones require a constant current power supply. The constant current signal conditioner built into the circuitry of the microphones contains a well regulated voltage source of 18 to 30 VDC that comes from a line-powered source[3]. This source is usually the data acquisition system as stated above. This is advantageous because fewer cables are needed with IEPE than with externally polarized microphones.

Despite the many advantages of IEPE microphones, they have a few drawbacks that likely contribute to the problems seen in the shock data. They can be limited in the high-frequency range by several different factors including the mechanical characteristics of the sensor, limitations on the amplifier or power supply, and by the characteristics of the cables used in the setup.

Mechanically, the sensitivity of a sensor increases rapidly as its natural frequency is approached. The natural frequency is given by

$$\omega = \sqrt{\frac{k}{m}} \quad (1.1)$$

where ω is the natural frequency, k is the stiffness constant of the sensor's sensing element, and m is the seismic mass. It is acceptable to be within a frequency bandwidth that causes the sensors sensitivity to deviate by no more than 5%. This occurs at about 20% of the resonance frequency[3]. The sensors in the microphones used have a large k value and low mass so the natural frequency is very high and therefore we don't need to worry about mechanical considerations in the system.

High-frequency problems can also arise from limitations in the amplifier or power supply of a sensor system. Problems generally occur after 100 kHz. These limitations are generally caused by capacitive filtering effects in the power supply[3]. Since we are not interested in frequencies that high, we don't need to worry about power supply limitations.

Problems can also occur in the high-frequency range due to cable specifications. Cables can be too long when the constant current is not sufficient to drive the capacitance in the cable. Distortion can occur for higher frequencies, shock waves, or transient testing in cables over 100 ft. Since cables used in rocket tests generally are 100 ft or longer this factor is important to consider. Equation 1.2 helps identify when signal distortion will occur.

$$F_{max} = \frac{10^9}{2\pi CV(I_c - 1)} \quad (1.2)$$

where F_{max} is the maximum frequency in hertz before distortion occurs, C is the total capacitance in picofarads, V is the maximum peak output voltage in volts, and I_c is the constant current provided by the system[3]. Figure 1.3 shows the maximum frequency against ratios of voltage to available constant current for several different cable capacitances.

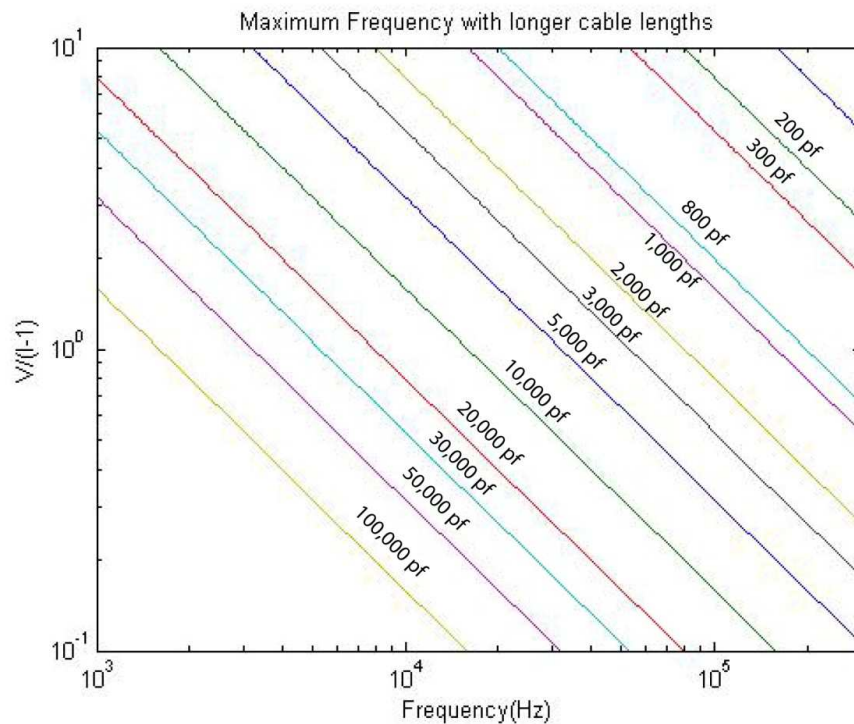


Figure 1.3 The curves show the maximum frequency at ratios of voltage over the current minus 1 before the signal is distorted for an ICP sensor using a longer cables for several different capacitance values[3]

IEPE microphones can also have problems in the low-frequency range that can attenuate the signal. These problems can arise from the discharge time constant of the microphone's sensor. IEPE microphones have capacitance that builds up a charge and creates a voltage when acted upon by a sound wave according to

$$\Delta V = \frac{\Delta q}{C_{Total}} \quad (1.3)$$

where ΔV is the voltage produced, Δq is the built-up charge, and C_{Total} is the capacitance of the microphone's sensor. Once a charge is built up it immediately begins to dissipate through the resistance in the microphone circuitry according to

$$Q = Q_0 e^{-t/RC} \quad (1.4)$$

where Q is the final charge, Q_0 is the initial charge, t is any time after the initial time, R is the resistance and C is the capacitance. The value RC is known as the discharge time constant[3]. Figure 1.4 is a plot of equation 1.4.

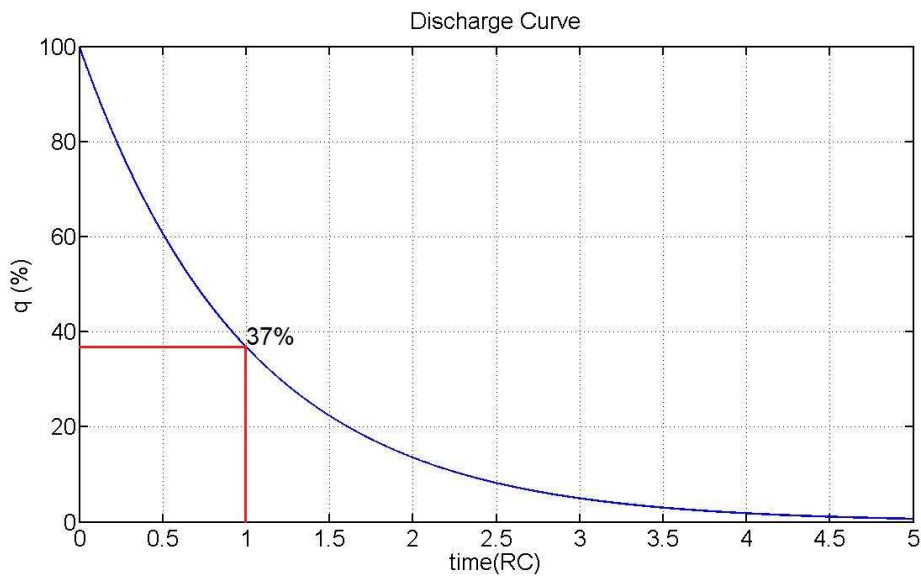


Figure 1.4 Plot of the discharge curve $q = Q_0 e^{-t/RC}$. Notice that after one discharge time has passed only 37 % of the charge remains.

The circuitry in an IEPE microphone is analogous to an RC high-pass filter for the lower frequencies, seen in Figure 1.5. This means that lower frequencies are attenuated as higher frequencies are allowed to pass[3]. In a high-pass filter if

$$f \ll \frac{1}{2\pi RC} \quad (1.5)$$

then the signal will be attenuated. When $f = \frac{1}{2\pi RC}$, f is known as the cutoff frequency.

If

$$f \gg \frac{1}{2\pi RC} \quad (1.6)$$

then the signal will pass through[5].

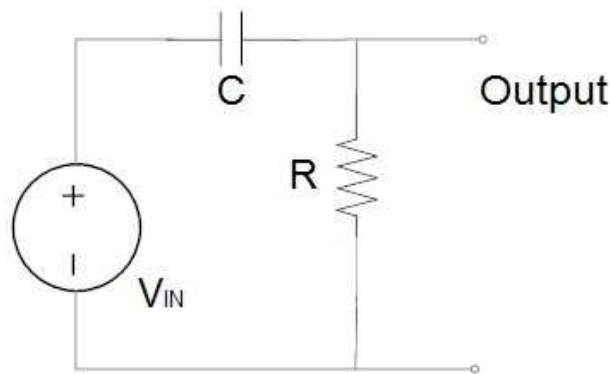


Figure 1.5 RC high-pass filter, similar to the circuitry in an IEPE microphone

Each microphone has a set RC value, so the discharge time constant cannot be changed. As will be discussed later in the results, the data in the low-frequency range were saturated, not attenuated. This means that the problem seen in

the data is not being caused by the high-pass filtering discussed here. It was brought up because there is a roll-off associated with normal microphone data in the low-frequency range. The data from the microphone systems that are having problems roll up in the low frequency range, which is not normal. Figure 1.6 illustrates this point with the power spectral density (PSD) data from the Orion-50 rocket test.

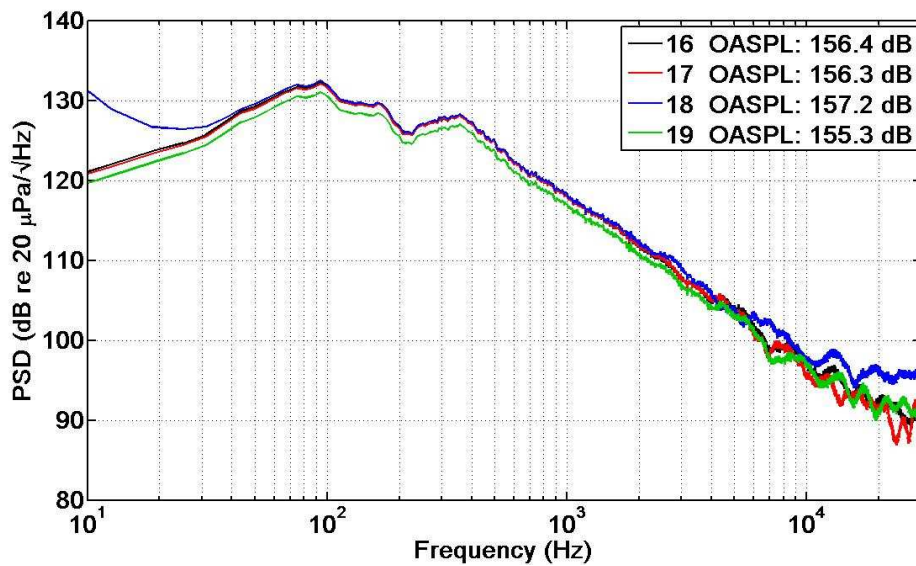


Figure 1.6 PSD from the Orion-50 rocket motor test. Notice that the data for one of the channels roll up in the low-frequency range, while the data of the other three channels roll off. The problems seen in the high-frequency range can be attributed to the problems discussed above. There is also low-pass filtering that affects the higher frequencies.

Chapter 2

Field Test

2.1 Equipment and Setup

The test was done with the objective of seeing which setups caused microphones to saturate and which did not. Setups that were used in previous tests, such as the Orion-50 test, that saturated were used again to see if saturation would happen again. The test consisted of three different stations. Stations one and three held four microphones each and station two held eight microphones using a machined microphone holder, and clamped to tripods. Figure 2.1 shows the microphone holder. It consists of two metal bars attached in a t-shape with the horizontal bar having alternating horizontal and vertical grooves that act as slots for holding the microphones. Three different types of microphones were used in the test. The first microphone was the GRAS 1/8" 40DD IEPE microphone used once in station one, twice in station two, and once in station three. The second microphone was the GRAS 1/4" 40BD IEPE microphone used once in station one, four times in station two, and three times in station three.

The third type of microphone was the GRAS 40BH ¼” microphone used once in station one and twice in station two.



Figure 2.1 Station 3 rig showing the microphone holder

The microphones were oriented in two different ways. Some were at normal incidence which is pointed directly at the plume. The others were at grazing incidence which is pointed 90° from the source, at the sky in this case. In an open area, pressure microphones will give the flattest response when they are at grazing incidence[6].

Stations one and three had two microphones at grazing incidence and two microphones at normal incidence. Station two had microphones at grazing incidence and six microphones at normal incidence. The microphones at normal incidence recorded higher pressure levels than the ones at grazing incidence; they were more likely to be saturated by the shocks since they were pointed directly at the source.

Figure 2.2 shows the curves from two adjacent microphones, one at grazing incidence and one at normal incidence, at a shock.

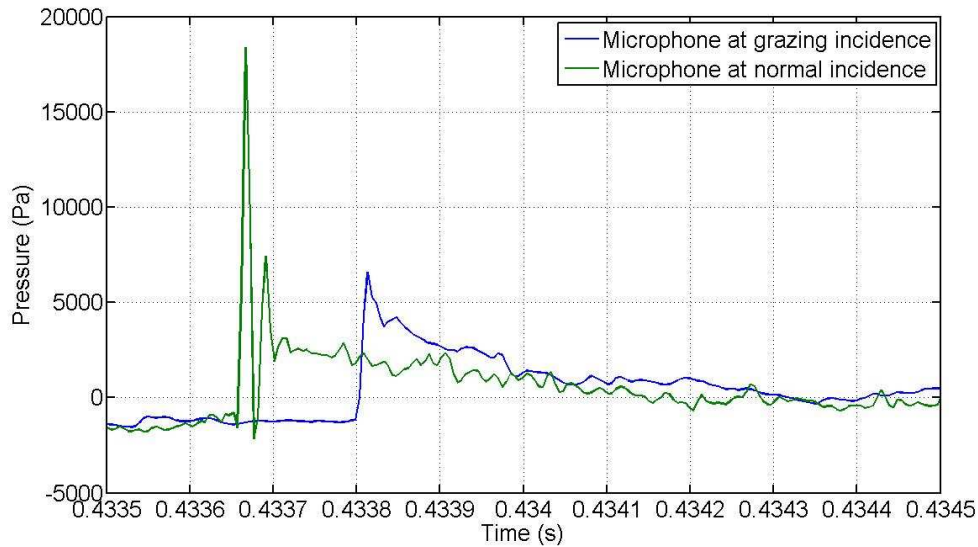


Figure 2.2 Shockwave recorded by two adjacent channels. The blue curve was oriented at grazing incidence and recorded a much lower pressure than the green curve which was oriented at normal incidence.

Different cables types were used to vary capacitance in each microphone system. The externally polarized microphones were connected to a GRAS 12AA power supply by a 7-pin LEMO cable. BNC cables ran from the output channels of the power supply. Some of the channels used microdot cables from the sensors that connected to BNC cables using a barrel connector. Three lengths of BNC cables were used. The RG-59 has a documented capacitance of 16.2 pF/ft, which is 1.62 nF for the 100 ft cables, 4.05nF for the 250 ft cables and 16.2nF for the 1000 ft cables. The measured capacitance of the 100 ft cables was about 2.3nF, the 250 ft cables was about 5nF and the 1000 ft cables was about 17nF. The ends of the cables are different for each one and can account for the slight differences in capacitance of what was measured and what is documented.

The other cable type that we used was the Spectra-Strip Skewclear 166-2699-997 infiniband cable. The infiniband cable consists of eight different cables bundled together in one cable. This cable is more convenient to use because only one cable, not several, need to be run from the sensors back to the data acquisition system. In previous tests, such as a test done with an Orion-50 rocket motor in 2010, some major problems have been seen in the data where infiniband cables were used. These problems are largely what motivated the KEI Stage-2 test. The infiniband cable is 250 ft long and has a measured capacitance of 2.7nF. The documented capacitance of the cable is 2.6nF[7], almost exactly what was measured.

The sensors with the RG-59 cables used 3m Microdot BNC cables that ran from the sensors to the RG-59 cables. The Microdot cables have a capacitance of .305nF. The RG-59 cables ran directly to a National Instruments (NI) PXI 4462 data acquisition card. The infiniband cable ran from a NI PXI 4498 data acquisition card to a NI BNC 2144 breakout box. 10 ft RG 174/U BNC cables with a capacitance of 16.2pF/ft ran from the breakout box to each of the sensors on the infiniband channels. Figure 2.3 shows the layout of an example station. Table 2.1 shows the sensor and cable type used for each channel at each station.

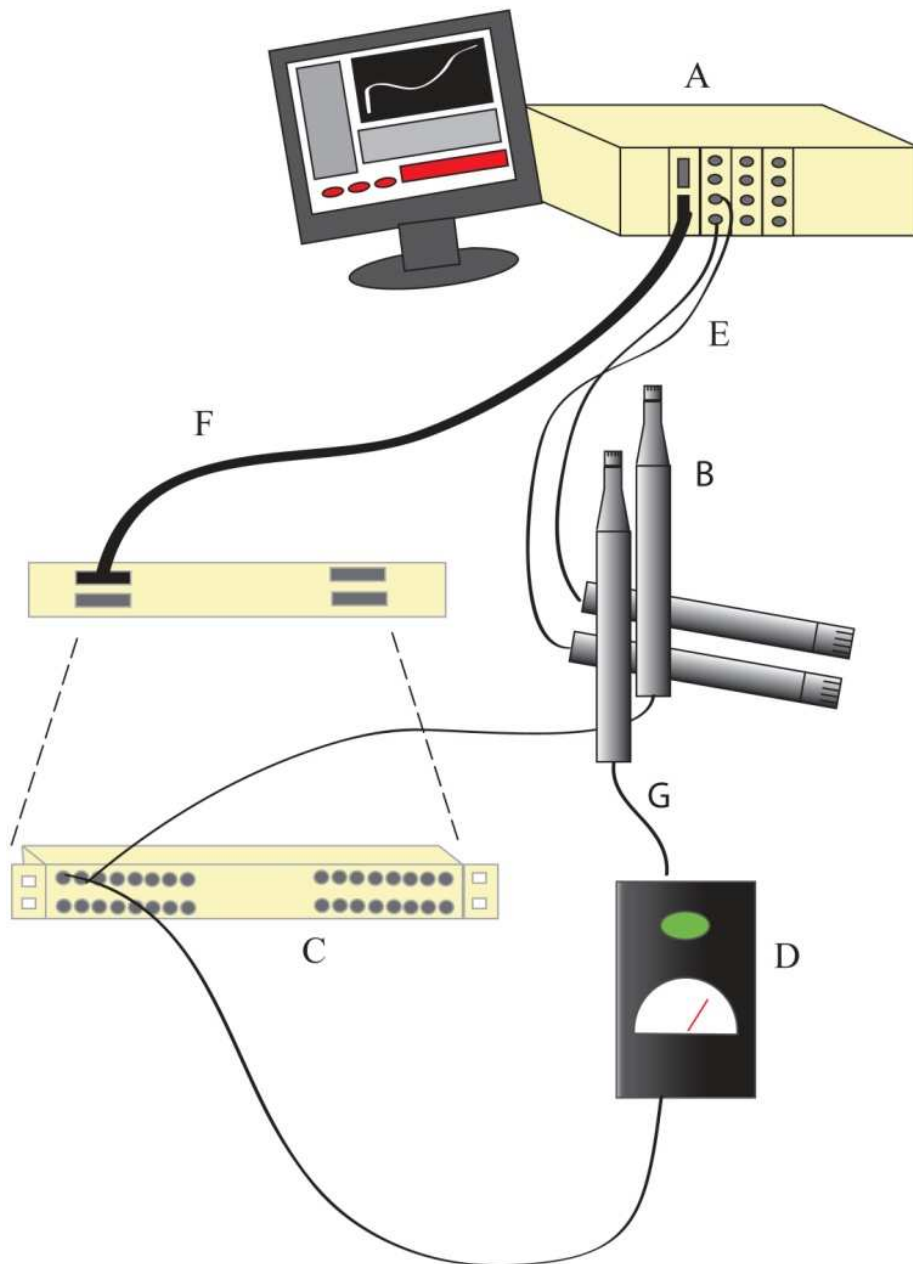


Figure 2.3 An example station of the setup at the KEI Stage 2 motor firing, including A) National Instruments (NI) PXI-1045 chassis holding NI PXI-4498 cards for the infiniband cable data acquisition and NI PXI-4462 cards for the BNC cable data acquisition B) 2 GRAS 1/8" microphones and pre-amplifiers at grazing incidence and 2 GRAS 1/4" microphones at normal incidence C) Front and Back of a NI BNC-2144 breakout box D) GRAS 12AA power supply E) Microdot cables from the microphones connected to BNC cables by barrel connectors F) Infiniband cable G) LEMO cable into power supply, BNC cable out of power supply

| Microphone Station Specifications | | | | | | |
|-----------------------------------|----------------|-------------|-------|-----------------------|-------------|-------------|
| Station Number | Channel Number | Sensor Type | Power | Cable Type and Length | Orientation | Sensitivity |
| 1 | 0 | 1/8" IEPE | 10 mA | 100 ft RG-59 | Grazing | 0.266 |
| | 1 | 1/4" IEPE | 4 mA | 100 ft RG-59 | Grazing | 0.491 |
| | 2 | 1/4" | 12AA | Infiniband | Normal | 0.469 |
| | 3 | 1/4" | 12AA | 100 ft RG-59 | Normal | 0.505 |
| 2 | 4 | 1/8" IEPE | 10 mA | 250 ft RG-59 | Grazing | 0.311 |
| | 5 | 1/8" IEPE | 4 mA | Infiniband | Grazing | 0.334 |
| | 6 | 1/4" IEPE | 10 mA | 250 ft RG-59 | Normal | 0.456 |
| | 7 | 1/4" IEPE | 4 mA | 250 ft RG-59 | Normal | 0.425 |
| | 8 | 1/4" IEPE | 4 mA | Infiniband | Normal | 0.456 |
| | 9 | 1/4" | 12AA | 250 ft RG-59 | Normal | 0.368 |
| | 10 | 1/4" | 12AA | Infiniband | Normal | 0.414 |
| | 11 | 1/4" IEPE | 4 mA | 1000 ft RG-59 | Normal | 0.368 |
| 3 | 12 | 1/8" IEPE | 10 mA | 250 ft RG-59 | Grazing | 0.327 |
| | 13 | 1/4" IEPE | 4 mA | 250 ft RG-59 | Grazing | 0.534 |
| | 14 | 1/4" IEPE | 4 mA | 1000 ft RG-59 | Normal | 0.501 |
| | 15 | 1/4" IEPE | 4 mA | Infiniband | Normal | 0.527 |

Table 2.1 A breakdown of the different microphone, cable, and orientation combinations used for the KEI Stage 2 rocket motor test

2.2 The Firing

The test took place at ATK Aerospace Systems in Promontory, UT on January 26, 2011 at 2:41 pm. The KEI missile is a land-based defense system capable of destroying enemy missiles in flight and features a high acceleration booster. It is a three stage missile that burns solid fuel. Stages one and two make up the propulsion system of the missile[8]. In this case Stage 2 was tested. The stage 2 motor of the KEI is a fast burning motor, lasting only about 30 seconds. It has an exit diameter of 23 1/8", so it was estimated that the plume would exit the motor in a 16° line. Station 1

was placed 31 ft in the horizontal or x direction and 21 feet in the vertical or y direction from the motor. Station 2 was placed 34.5 ft in the x direction and 32 feet in the y direction. Station 3 was placed 47 ft in the x direction and 74 ft in the y direction, as shown in the diagram in Fig 2.4.

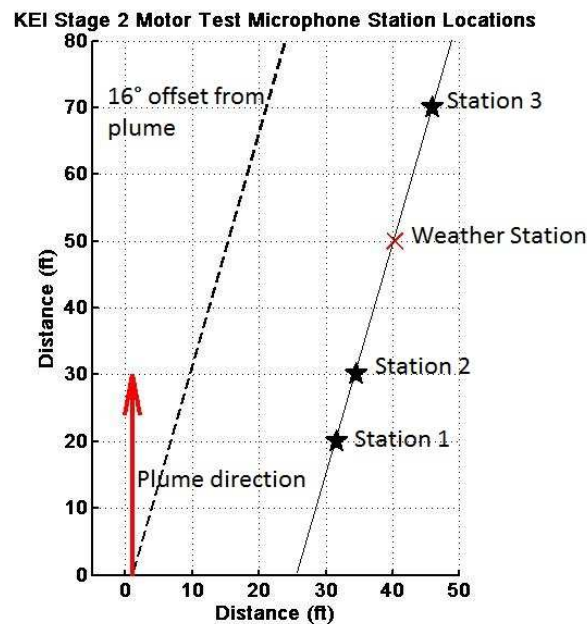


Figure 2.4 Station locations of the KEI Stage 2 rocket motor test

The weather conditions were recorded before, during and after the test. The temperature before the test started was 4.99 °C. The temperature rose to 8.3 °C during the test and steadily fell back down to 4.99 °C over a period of 11.5 minutes after the test. Figure 2.5 shows the relative humidity just before, during and after the test, the test takes place from about $t=2s$ to $t=32s$ on the graph. The humidity dropped by 10% once the test started and slowly climbed back up after the test was over. This is because the rocket fire dried out the air. Figure 2.6 shows the air pressure just before

and during the test. Once again, $t=2s$ to $t=32s$ is when the test took place. The pressure was at 87.2 kPa just before the test and rose and dropped between 87 and 87.5 kPa during the test. After the test the pressure settled back to 87.2 kPa.

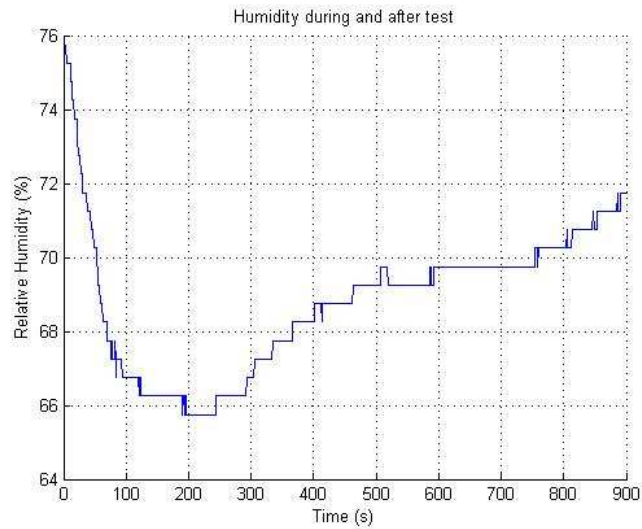


Figure 2.5 Relative humidity data for just before, during and after the rocket motor firing.

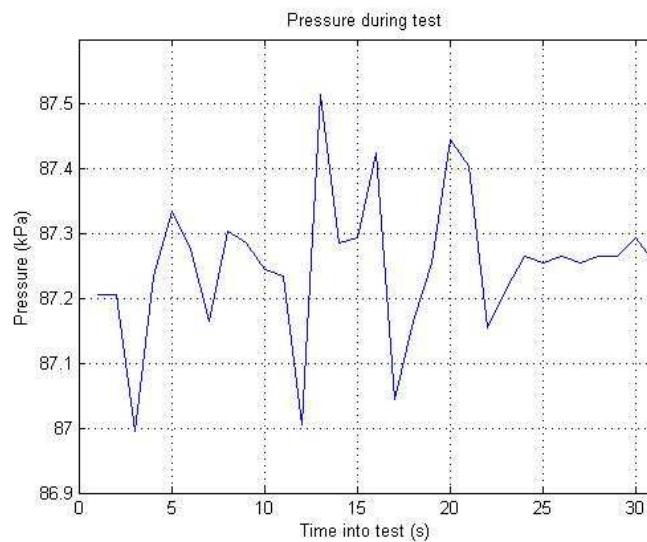


Figure 2.6 Air pressure just before and during the rocket motor firing.

Figure 2.7 shows the wind speed in m/s and direction during the test. 0° was along the line of the microphones (see Fig. 2.3). The wind speed varied from 1.5 m/s and 3 m/s at directions varying from 190° to 250° from the microphone line.

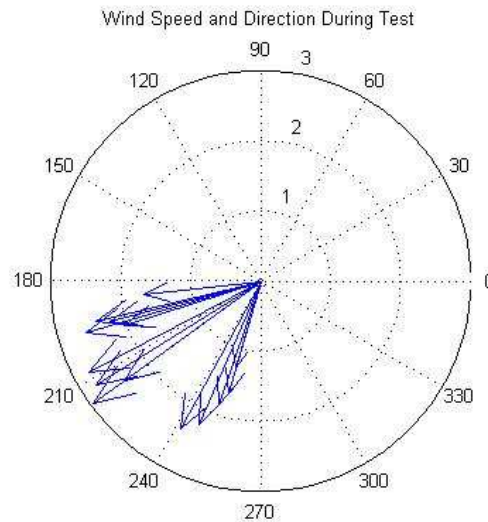


Figure 2.7 Wind speed in m/s and direction during the rocket motor firing.

The microphones were set to record data for ten minutes, beginning 5 minutes before the test was scheduled to begin and ending five minutes after the test was scheduled to begin. Time waveform data were recorded simultaneously for each channel on NI PXI 4462 data acquisition cards for the channels on BNC cables and on NI PXI 4498 data acquisition cards for the channels on infiniband cables at a sampling rate of 204.8 kHz. Figure 2.8 shows a picture of the test pad, rocket motor, and the microphone stations.



Figure 2.8 The KEI Stage 2 rocket motor, test pad, test bay and microphone stations. Station 1 is the station nearest the motor. The next station is Station 2, followed by the weather station and the station nearest the camera is Station 3.

Chapter 3

Results and Analysis

3.1 Data

Figures 3.1, 3.2 and 3.3 show the power spectral densities (PSD) for Stations 1, 2 and 3 respectively taken from the KEI test. At Station 1 the measured data was typical data from rocket noise fields. All four channels have the same PSD form with about the same decibel levels, as seen in Figure 3.1. At station 2, channels 7, 8 and 11 showed problems in the data, as seen in Figure 3.2 in the PSD where the data rolls up in the lower frequency range. All three of these channels were powered by 4 mA of constant current. Channel 11 shows the worst problems at this station. The major difference between channel 11 and channels 7 and 8 is that channel 11 used a 1000 ft RG-59 cable, 7 used a 250 ft RG-59 cable and 8 used an infiniband cable.

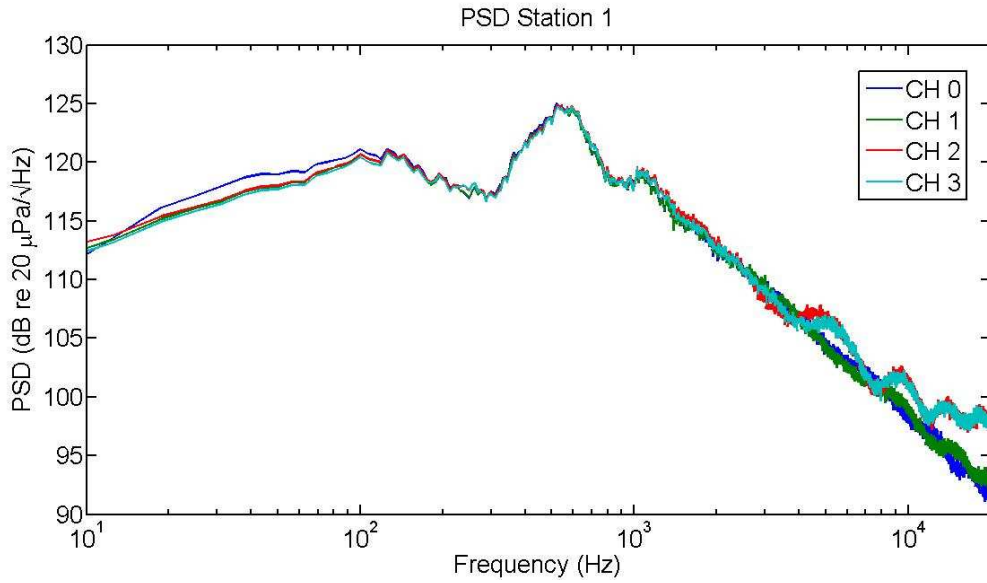


Figure 3.1 PSD for Station 1

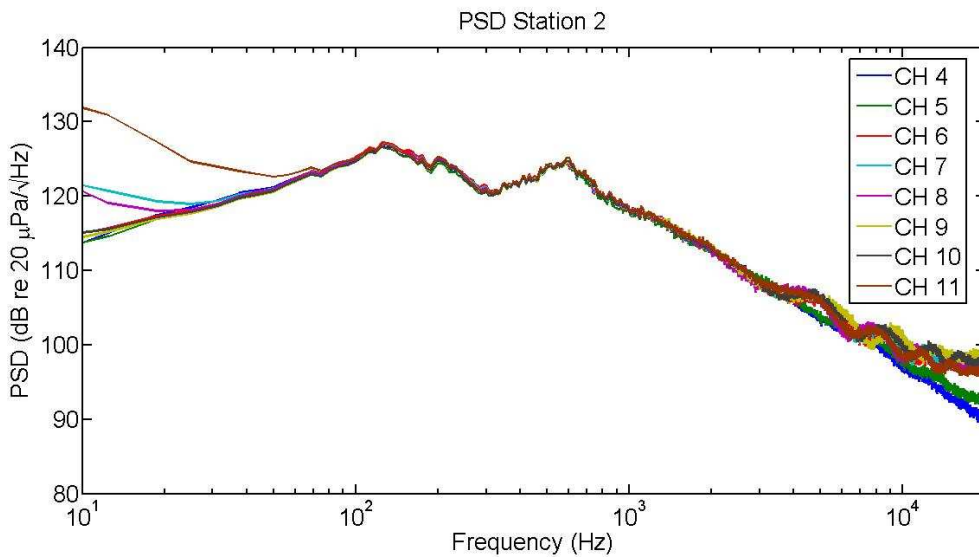


Figure 3.2 PSD for Station 2

At station 3, channels 13, 14, and 15 all showed problems as seen in Figure 3.3. Channel 14 showed the worst problems at this station. Channel 14 used the 1000

ft RG-59 cable, channel 13 used a 250 ft RG-59 cable and channel 15 used an infiniband cable. Also, just as was the case with station 2, all three of the problem channels at station 3 received 4 mA constant current.

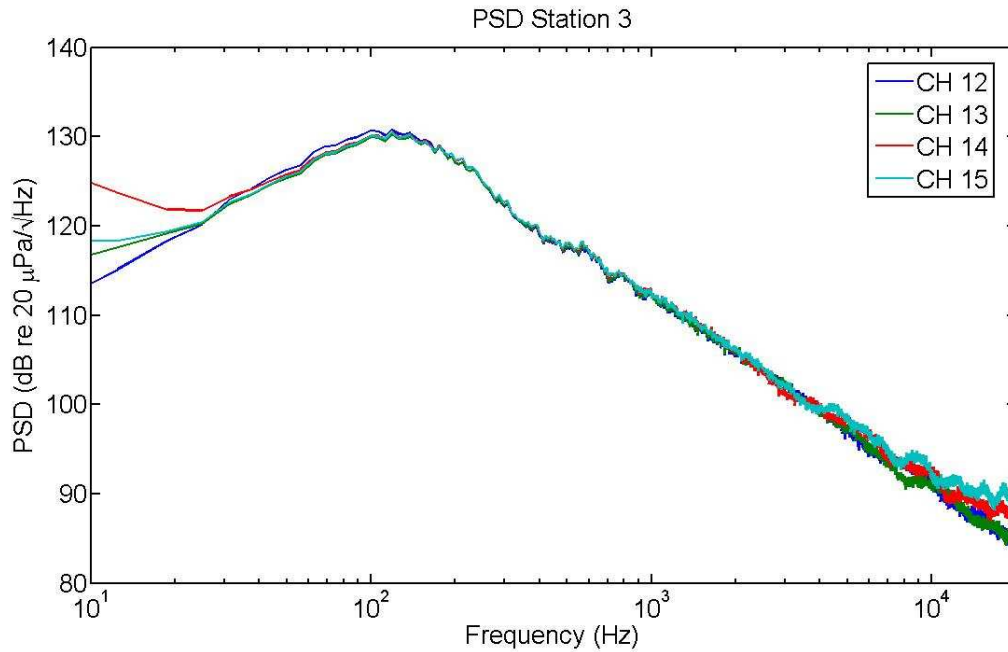


Figure 3.3 PSD for Station 3

3.2 Analysis

After talking to a representative at GRAS, the manufacturer of the microphones that we use in our experiments, we came to the hypothesis that a capacitor is discharging somewhere in the system that is causing the data to not reach the pressure levels it should be when the shocks occur. If this were indeed the case, then the systems with the highest capacitance would show the greatest problems. In our setup, the variable

that would cause the greatest difference in the capacitance among the different channels was the cable type used. However, our results showed that this is only partially correct as the cables with the lowest capacitance, the infiniband cables, still showed problems.

All of the channels that saturated were supplied with 4 mA of current. However, not all channels that were supplied with 4 mA had problems, so it is important to also look at other factors. Both channels that used 1000 ft RG-59 cables showed the most problems, so low current with a high capacitance causes the worst problems. Channels 1 and 5 didn't have any problems but were only supplied with 4 mA of current; but they were oriented at grazing incidence. Channel 13 was supplied with 4 mA and was oriented at grazing incidence like channels 1 and 5. However, it did show problems. The difference is that it used a 250 ft RG-59 cable therefore it had a higher capacitance than channels 1 and 5. Channel 13 also had the highest sensitivity of any of the microphones at .534 mV/Pa. It is possible that sensitivity along with low current and higher capacitance may play a factor.

In these systems:

$$I = C \left(\frac{dV}{dt} \right) \quad [9] \quad (3.1)$$

This tells us that when there are large shocks, the $\frac{dV}{dt}$ in equation 3.1, and large capacitances, more current is needed. At two shockwaves, the $\frac{dV}{dt}$ values of a microphone that saturated were compared to the $\frac{dV}{dt}$ values of an adjacent microphone with the same orientation that did not saturate. Figure 3.4 shows an example of two

adjacent channels at the same orientation where the green curve saturated and the blue curve did not.

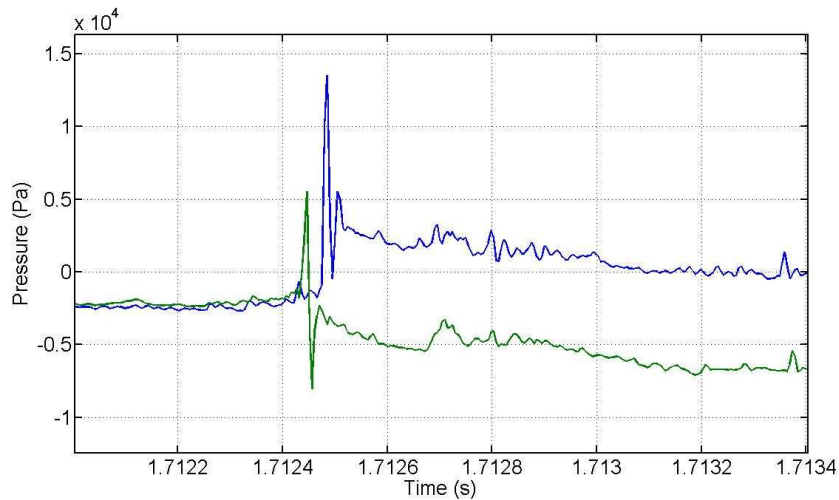


Figure 3.4 An example of a shockwave recorded by two adjacent channels at the same orientation. The green curve saturated while the blue one did not.

This will show the $\frac{dV}{dt}$ values that the saturated microphone achieved compared to the $\frac{dV}{dt}$ values it should have achieved. Even though channels 14 and 15 saturated, they were not used in this analysis since neither channel had an adjacent channel that did not saturate. Table 3.1 shows the $\frac{dV}{dt}$ values for the pairs of microphones. The rows highlighted in red indicate that channel saturated. Note that all the saturated channels saturated at about the same $\frac{dV}{dt}$ value both times. Channel 11 on the 1000 ft RG-59 cable had the lowest $\frac{dV}{dt}$ values and the data showed that it had the worst saturation levels. Channel 8 on the infiniband cable had the highest $\frac{dV}{dt}$ values, and the data usually showed the least saturation on the channels with infiniband.

| Channel | dV/dt #1 (V/ μ s) | dV/dt #2 (V/ μ s) |
|---------|-------------------------|-------------------------|
| 6 | 0.407 | 0.3 |
| 7 | 0.276 | 0.262 |
| 8 | 0.308 | 0.286 |
| 9 | 0.327 | 0.342 |
| 10 | 0.434 | 0.33 |
| 11 | 0.127 | 0.116 |
| 12 | 0.154 | 0.108 |
| 13 | 0.147 | 0.145 |

Table 3.1 At two different shockwaves, $\frac{dV}{dt}$ levels for four of the channels that saturated compared to an adjacent microphone of the same orientation that did not saturate. The rows highlighted in red indicate that channel saturated.

It is interesting to note that channel 13 saturated at a higher $\frac{dV}{dt}$ value than channel 12 achieved in case 2. This is because channel 13 had a much higher sensitivity than channel 12. In all the other cases, the sensitivities of the two microphones were relatively close. Although the results are consistent, they are unique to each setup. If the total capacitance of a system is known, Equation 3.1 can be used to determine the largest $\frac{dV}{dt}$ a system can handle for a given current without saturation.

It is useful to compare the KEI Stage 2 test to the Orion-50 test done previously. The setup of the Orion-50 test consisted of several tetrahedral probes, some encased in spheres and some mounted on external frames as seen in Figure 3.5. There were also a few single microphones set up at grazing incidence. All channels were IEPE microphones and received 4 mA constant current. The only microphones that saturated in this test were on channels that utilized the infiniband cables and were

not at grazing incidence. All of the channels on RG-59 cable were at grazing incidence. For the Orion-50 test, it seems that the deciding factor of whether a microphone would saturate or not was whether it was at grazing incidence or some other orientation since all channels received 4 mA of current. However, not all microphones at some other orientation saturated.

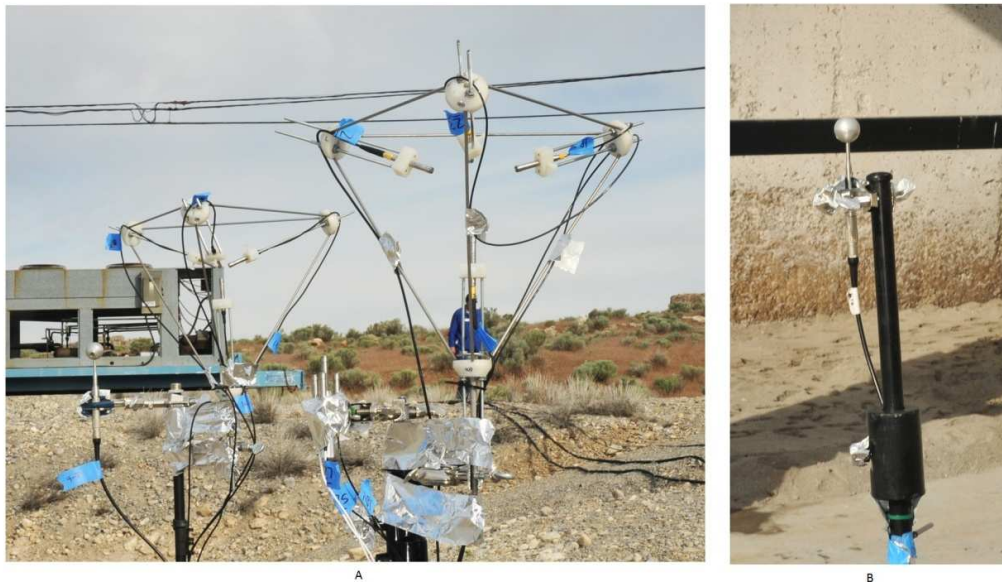


Figure 3.5 A) External frame tetrahedral probes and B) Tetrahedral probes encased in a sphere

Table 3.2 shows pressures and voltages at shockwaves for nine channels that saturated during the Orion-50 test. Unfortunately, the same analysis of the $\frac{dV}{dt}$ levels done for the KEI test is not possible for the Orion test since adjacent channels were not at the same orientation.

| Channel | Pressure kPa | Voltage (V) |
|---------|--------------|-------------|
| 1 | 19.26 | 5.4 |
| 3 | 11.91 | 3.1 |
| 4 | 7.84 | 3.0 |
| 7 | 8.43 | 2.3 |
| 9 | 17.06 | 4.8 |
| 11 | 7.72 | 3.2 |
| 18 | 9.62 | 3.4 |
| 22 | 15.65 | 6.7 |
| 32 | 6.25 | 5.8 |

Table 3.2 Pressure and voltage at a shockwave of nine channels that saturated during the Orion-50 test.

In another correspondence with GRAS, we were told that the data acquisition card can also have an effect on the data. The PXI 4462 cards, where all the RG-59 cables connected into, are older models and do not have as high of a bandwidth as the newer PXI 4498 cards, where all the infiniband cables connected into. Because of the higher bandwidth in the circuitry of the 4498 cards, they can handle shocks better on systems with higher capacitances and lower currents than can the 4462 cards[9]. This explains why the infiniband cable channels still saturated when they only had 4 mA constant current, but did not saturate as severely as the channels on the RG-59 cables with 4 mA of current.

Chapter 4

Conclusion

Conditions of when a channel will saturate were established. Channels never showed saturation when they were supplied with 10 mA or an externally polarized microphone powered by a 12AA power supply was used. Generally, setting a microphone at grazing incidence will not saturate the microphone, but this is not always the case when 4 mA is used. Supplying a channel with 4 mA on a 1000 ft RG-59 causes the worst saturation. The best conditions for non-saturation on IEPE channels are setting the microphones at grazing incidence, using 10 mA current, and using an infiniband cable because it has the lowest capacitance and utilizes the PXI-4498 card with the high bandwidth.

Using Equation 3.1, with a given current and a known system capacitance, it can be determined what $\frac{dV}{dt}$ values a system can handle before it saturates. The $\frac{dV}{dt}$ levels were established for the specific systems used in the KEI Stage 2 rocket motor test, but these are unique for each system which can vary by microphone type, cable

type and length, and amount of power supplied to the system. Future work will include more tests with these systems to see if the $\frac{dV}{dt}$ levels established here are consistent.

Bibliography

- [1] Gee, K.L., et al., "Energy-Based Acoustical Measurements of Rocket Noise", in 15th AIAA/CEAS Aeroacoustics Conference (30th AIAA Aeroacoustics Conference). 2009: Miami, Florida.
- [2] Kinsler, L.E., et al., *Fundamentals of Acoustics Fourth ed.* 2000, New York: Wiley.
- [3] PCB Group. Tech guide for ICP Sensors. 2011; Available from: http://pcb.com/techsupport/tech_signal.php.
- [4] PCB Piezotronics, Inc. "Microphone Handbook Test and Measurement Microphones". Available from: http://www.pcb.com/Linked_Documents/Vibration/Microphone_handbook.pdf.
- [5] Moura, L. and I. Darwazeh, *Introduction to Linear Circuit Analysis and Modelling.* 2005, Oxford: Newnes.
- [6] Schneider, A.J., "Microphone orientation in the sound field." *Sound Vibration*, 1970. 4(2): p. 20-25.
- [7] Holliman, M., Spectra-strip representative (private communication)
- [8] Staff writers, Northrop Grumman "KEI Team Completes Fourth Rocket Motor Test", in *Globe Newswire*. 2007: Promontory, UT.
- [9] Piazza, C., GRAS representative (private communication)